RESEARCH ARTICLES

Direct numerical simulation of the initial evolution of a turbulent axisymmetric wake

A. J. Basu*, R. Narasimha*† and U. N. Sinha*

*National Aeronautical Laboratory, Bangalore 560 017, India
*†Jawaharlal Nehru Centre for Advanced Scientific Research, Indian Institute of Science Campus, Bangalore 560 012, India

The initial evolution of a turbulent axisymmetric wake at a macroscale Reynolds number of 1500 has been simulated by direct solution of the unsteady three-dimensional Navier–Stokes equations using a (temporal) spectral scheme on the Flosolver Mk3 parallel computer at NAL. A visualization of the flow is presented in terms of constant-vorticity surfaces. The simulation shows a complete sequence of events from formation of vortex rings through generation of azimuthal instability and appearance of streamwise structures to eventual breakdown into turbulent flow, and reveals explicitly certain interesting features of the development of streamwise vorticity.

TURBULENT flows continue to provide the greatest challenge in studies of fluid dynamics, in spite of more than a century of scientific effort that has resulted in the acquisition of enormous amounts of experimental data and the formulation of many theoretical approaches[1]. The chief reason for the lack of any satisfactory theory to-date is that the Navier–Stokes equations that govern turbulent flows are nonlinear, and no exact solutions are known that may be relevant to an understanding of turbulence for any geometry. Experimental studies have thrown considerable light on various aspects of turbulence phenomena, but not all physical variables of interest are accessible to available instrumentation. Among the most prominent of these is the vorticity vector, whose three components are difficult to measure, especially with the resolution required to acquire the finest viscous scales. Complete measurements of such vector fields over a three-dimensional domain are till today virtually impossible.

When feasible, direct solution of the full, unsteady, three-dimensional Navier–Stokes equations (which we shall abbreviate to DNS, often also standing for direct numerical simulation), can provide the kind of complete data that experiments cannot. In particular, such simulations yield instantaneous pictures of any flow variable over the whole computational domain, but are very demanding on computer power and memory because of the need to resolve the wide range of length and time-scales encountered in turbulent flows (see Reynolds[2] for a recent review: the ratio of scales to be resolved increases like the 3/4 power of the Reynolds number (Re) of the flow). At present, DNS is usually performed on 64^3 or 128^3 grids, although 256^3 and 512^3 grids have been occasionally attempted. If N is the number of grid points along any space direction, then the number of operations per time-step[3] is typically of the order of

$$75\,N^3 \log_2 N + 100\,N^3.$$

For a 100 MFLOPS computer with careful programming, the CPU time required per time-step for homogeneous turbulent flow simulation is about 3 minutes at a Reynolds number (based on the turbulent macroscale and velocity scale) of 100, and 9 hours at a Reynolds number of 400. A typical simulation of fully developed turbulent flow takes 5000 or more time-steps. It is thus clear that such simulations need substantial computing power, and have been attempted only where super-

computers are easily available, most notably in the US, Germany, Japan and France.

With the availability of the third generation (Mk3) of the parallel computers in the Flosolver series developed at the National Aeronautical Laboratory (NAL), the computational power needed to undertake such a project has now become available in India[4,5]. The purpose of the present article is to demonstrate one such direct Navier–Stokes solution for the interesting problem of an axisymmetric turbulent wake, and to present preliminary answers to certain important questions about vorticity generation in the flow.

The evolution of an axisymmetric wake has long posed some intriguing questions of both fundamental and practical significance. It is well known that a wake breaks down to turbulence at relatively low Reynolds numbers, in particular when the body producing the wake has salient edges from which thin shear layers can emerge in the flow. A classical approach to fully turbulent flow seeks the so-called self-preserving solutions, which predict for the axisymmetric wake (as discussed by Townsend[6], for example) that the thickness δ of the wake and the maximum velocity defect w_0 (Figure 1) vary with downstream distance z as

$$\delta \sim z^{1/3}, \qquad w_0 \sim z^{-2/3}.$$

These relations have been supported by the experiments of Hwang and Baldwin[7]. It will immediately be seen that the local Reynolds number of the flow, $\mathrm{Re} \equiv w_0\,\delta/\nu$ (ν is the kinematic viscosity), decreases with distance like $z^{-1/3}$. Thus, while the wake undoubtedly achieves a fully turbulent state fairly close to the body at even modest Reynolds numbers, it would appear that it should revert to the laminar state sufficiently far downstream! Although the approach to the laminar state should be extremely slow because it is dissipative (see Narasimha and Sreenivasan[8] for a discussion of this point), the possibility of a single flow that encompasses instability, transition to turbulence, a more or less mature turbulent state and eventual relaminarization offers a rich variety of phenomena to comprehend. There is also the important question of the extent to which the wake remembers the body that generates it. This question is not only of fundamental significance in turbulence, but has practical importance in attempts to detect the presence and characteristics of a body by sensing its far downstream wake.

From the computational point of view, the axisymmetric wake has the convenient property that (because its Reynolds number decreases downstream) the demands on resolution will also diminish with flow development, in contrast to most other flows that have been investigated so far.

For all these reasons an axisymmetric wake is an intriguing flow whose exact simulation promises to throw much light on a variety of questions. We confine our attention in this article to the generation of three-dimensional vorticity as the flow breaks down into turbulence.

The spectral scheme

Of various methods used for direct numerical simulation of turbulence, the spectral method has the

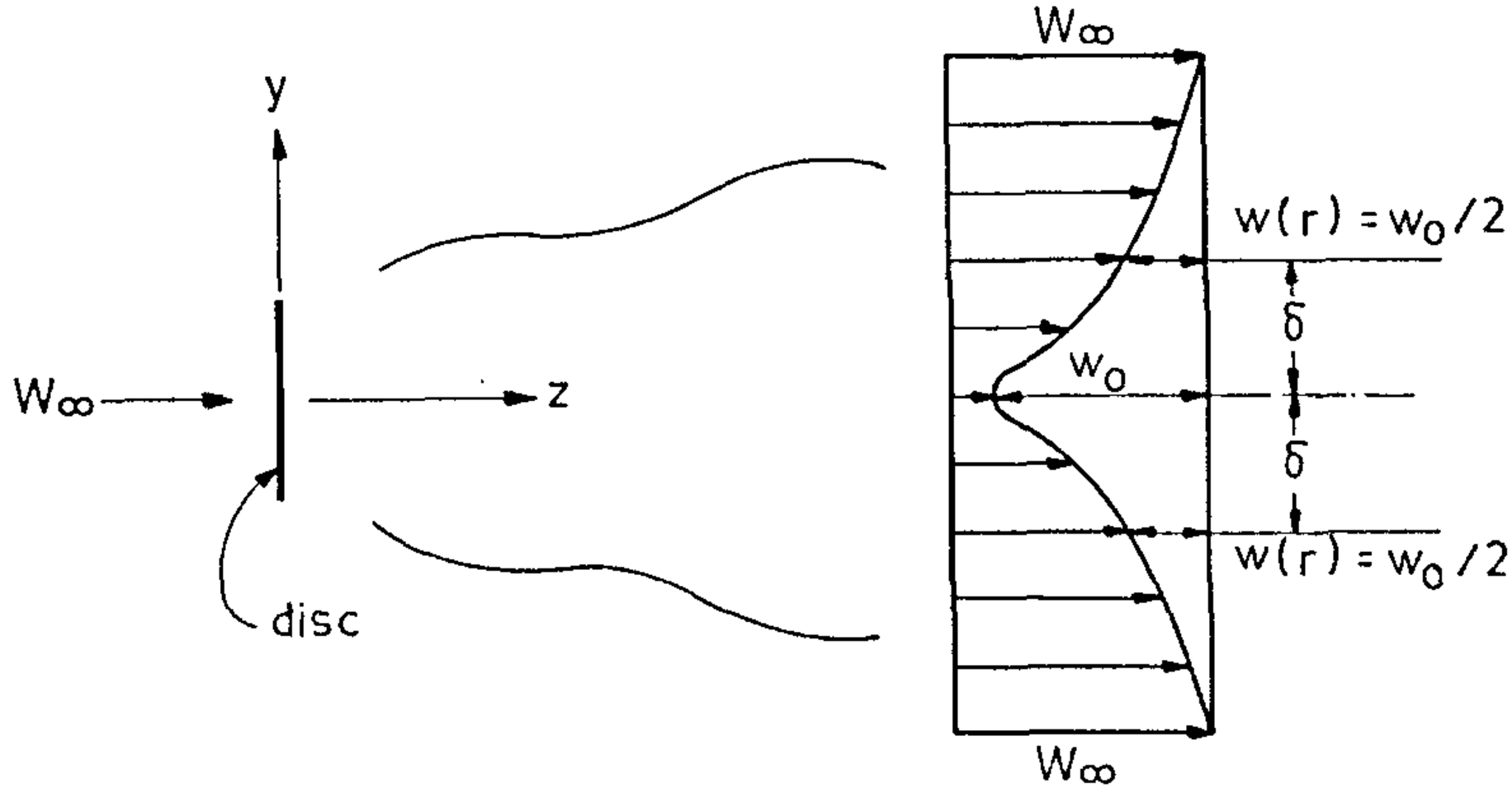

Figure 1. A sketch of a typical three-dimensional axisymmetric wake behind a disc. The flow is along z. The mean streamwise velocity and the velocity defect profiles are shown on the right.

advantage of rapid convergence because of the exponential decay of errors (compared to algebraic decay in the finite-difference method, for example), but is difficult to adopt for complicated geometries. For the simulation of transitional flows accuracy is not a luxury but a necessity[2], so the spectral scheme is to be preferred. It has been extensively treated by Canuto *et al.*[3]; the method that we shall adopt, first proposed by Orszag[9], will be briefly described here.

The Navier-Stokes equations for the flow of an incompressible fluid in three dimensions can be written as

$$\frac{\partial}{\partial t}\mathbf{v}(\mathbf{x},t)+\mathbf{v}(\mathbf{x},t)\cdot\nabla\mathbf{v}(\mathbf{x},t)=-\nabla p(\mathbf{x},t)+\nu\nabla^2\mathbf{v}(\mathbf{x},t), \tag{1a}$$

$$\nabla\cdot\mathbf{v}(\mathbf{x},t)=0, \tag{1b}$$

where $\mathbf{v}(\mathbf{x},t)=(v_1,v_2,v_3)$ is the velocity field in a three-dimensional space defined by the vector $\mathbf{x}=(x_1,x_2,x_3)$ and p is the pressure normalized by density. We choose a boundary condition with a period 2π in all three space directions, so that

$$\mathbf{v}(\mathbf{x}+2\pi\mathbf{e},t)=\mathbf{v}(\mathbf{x},t), \tag{2}$$

where $\mathbf{e}=(e_1,e_2,e_3)$, $e_\alpha=0,\ \pm1,\ \pm2,\ldots$, for $\alpha=1,2,3$. Given an initial condition such as

$$\mathbf{v}(\mathbf{x},0)=\mathbf{v}_0(\mathbf{x}), \tag{3}$$

the problem is to compute the evolution of $\mathbf{v}(\mathbf{x},t)$ and $p(\mathbf{x},t)$.

The solutions are written in the form of the Fourier expansions

$$\mathbf{v}(\mathbf{x},t)=\sum_{k\le K}\mathbf{u}(\mathbf{k},t)e^{i\mathbf{k}\cdot\mathbf{x}}, \tag{4a}$$

$$p(\mathbf{x},t)=\sum_{k\le K}q(\mathbf{k},t)e^{i\mathbf{k}\cdot\mathbf{x}}, \tag{4b}$$

where $\mathbf{k}=(k_1,k_2,k_3)$ is an integer wavevector, $k^2=k_\alpha k_\alpha$, $K=N/2$ is a finite cut-off, and $k\le K$ means $-K\le k_\alpha\le K$ for $\alpha=1,2,3$; $\mathbf{u}(\mathbf{k},t)$ and $q(\mathbf{k},t)$ are the Fourier- (or $\mathbf{k}$-) space representations of $\mathbf{v}(\mathbf{x},t)$ and $p(\mathbf{x},t)$ respectively. The Navier–Stokes equations in Fourier-space can then be written as

$$\frac{\partial}{\partial t}\mathbf{u}(\mathbf{k},t)=-ik\,q(\mathbf{k},t)-[\mathbf{v}(\mathbf{x},t)\cdot\nabla\mathbf{v}(\mathbf{x},t)]_k-\nu k^2\mathbf{u}(\mathbf{k},t), \tag{5a}$$

$$i\,\mathbf{k}\cdot\mathbf{u}(\mathbf{k},t)=0, \tag{5b}$$

where the subscript k is used to imply that the entire expression within the brackets is to be evaluated in the Fourier space. Using the incompressibility condition ((equation (5b)), we can eliminate the pressure term from equation (5a), and obtain[9] along any space direction $\alpha(\alpha=1,2,3)$

$$\frac{\partial}{\partial t}u_\alpha(\mathbf{k},t)=-\nu k^2u_\alpha(\mathbf{k},t)-\frac{i}{2}P_{\alpha\beta\gamma}(\mathbf{k})\sum_{\substack{\mathbf{m}+\mathbf{n}=\mathbf{k}\\ m,n\le k}}u_\beta(\mathbf{m},t)u_\gamma(\mathbf{n},t), \tag{6}$$

$$k_\alpha u_\alpha(\mathbf{k},t)=0, \tag{7}$$

where

$$P_{\alpha\beta\gamma}(\mathbf{k})=k_\beta(\delta_{\alpha\gamma}-k_\alpha k_\gamma/k^2)+k_\gamma(\delta_{\alpha\beta}-k_\alpha k_\beta/k^2), \tag{8}$$

and the repeated Greek subscripts are summed over the range 1, 2, 3.

The convolution sums $\Sigma u_\beta u_\gamma$ in equation (6) are responsible for all the complexities of the spectral scheme. To compute such terms accurately in Fourier-space using matrix-multiplication is very time-consuming. In an alternative device due to Patterson and Orszag[10], which simplifies this calculation, the components of the above convolution sums in $\mathbf{k}$-space are first transformed using Fast Fourier Transforms (FFTs) to physical- (or $\mathbf{x}$-) space where the multiplications are performed; the results are then transformed back to $\mathbf{k}$-space again using FFTs. Because of the high speed of FFTs, this entire operation can be done significantly faster this way than through matrix-multiplication in $\mathbf{k}$-space.

This method suffers from the difficulty that the computed convolution sum, when transformed back to $\mathbf{k}$-space, has 'aliasing errors' that result from the truncation of an essentially infinite Fourier series to a finite number of terms[3,9]. Fortunately, these errors can be removed completely by certain special techniques, of which the '2/3rd rule'[3] has been used here. This involves truncation in $\mathbf{k}$-space so that only such wavenumbers for which

$$k<(2/3)K, \tag{9}$$

are retained.

For integrating in time, we have used a third-order accurate Runge–Kutta scheme to start the computation, followed by a predictor–corrector scheme for further time-integration.

In what follows we shall use cylindrical (r,ϕ,z) or Cartesian $(x=r\cos\phi,\ y=r\sin\phi,\ z)$ coordinate systems as convenient. The corresponding velocities are (v_r,v_ϕ,w) and (u,v,w) in the two systems.

The initial conditions are set up such that we have a

tubular shear layer at time $t=0$, with a top-hat velocity profile across the thickness σ of the tube, given by

$$\begin{aligned} w &= W_x && \text{for } r \geq r_0+\sigma/2 \\ &= 0 && \text{for } r \leq r_0-\sigma/2 \\ &= (W_x/2)\,(1+\tanh\,((r-r_0)/2\theta)) && \text{for } r_0-\sigma/2<r<r_0+\sigma/2, \end{aligned} \tag{10}$$

and $\tanh\,(4\sigma/\theta)\approx 1$; W_x is the free-stream velocity, r_0 is the initial radius of the wake and θ is the momentum thickness of the shear layer. We impose a small perturbation on this shear layer corresponding to an increment in the radial component of velocity v_r given by

$$\Delta v_r = a_z \sin(mz+\psi_z)+a_\phi \sin(n\phi+\psi_\phi), \tag{11}$$

with prescribed amplitudes a_z and a_φ and phases ψ_z and ψ_ϕ. In the present computations, we have put in three streamwise modes (corresponding to $m=1$, 2 and 4) and the first 16 azimuthal modes, all the latter with very small amplitudes and random phases.

The free-stream velocity at $t=0$ is $W_x=1$, and the centreline velocity defect w_0 is also equal to 1. The computations are made in double precision on a 64^3 grid, the computational domain having the size 2π in all three directions.

Parallelization

The spectral algorithm for solving the Navier-Stokes equations cannot be parallelized profitably using the domain-decomposition technique[11], so effectively used with the finite-difference and finite-element methods. One option is to parallelize the FFTs themselves, since they constitute a sizeable fraction of the calculations. This approach is most appropriate for butterfly-connected parallel machines such as NCUBE, on which Pelz[12] parallelized a spectral algorithm this way. However, the approach does not distribute the memory requirement equally between processors, and so is wasteful on the Flosolver in which the available memory *is* evenly distributed.

The ease of parallelizing matrix-multiplication on some machines, especially with a large number of processors, has led to the adoption of matrix multiplication by some previous investigators[13,14] to compute the convolution sums in equation (6). On a multi-computer with a small number of processors such as the Flosolver, however, matrix-multiplication is inefficient compared to the FFT-based algorithm of Orszag.

Keeping in mind these factors, we have chosen to develop an algorithm that distributes the memory requirement and the computing load equally between different processors, thus easing the process of bus-synchronization[15,16]. This algorithm computes the evolution of each of the three velocity components in a different processor. The evolution of any velocity component is of course not independent of the others because of nonlinearity, and hence a certain amount of data transfer between different processors is necessary. In the present computations, this transfer is made in large blocks, and is a fast operation due to the presence of dedicated message-passing co-processors in the Flosolver architecture. As a consequence, most of the time could be devoted to the actual computation itself, and a parallelization efficiency of up to 97% has been achieved. The finer details of the parallel algorithm have been published separately[15,16] and will not be repeated here.

Kerr[17] performed similar calculations on a single-processor Cray-XMP for isotropic turbulence, and reports a CPU time of 3.25 s per time step. Using the present algorithm and the same time-stepping scheme as Kerr, the CPU time is about 8 s on the 3-processor Flosolver Mk3, i.e. the sustained computational performance is about 40% of that of the Cray-XMP[15]. It will be possible to attempt finer grids (and higher Reynolds numbers) in future as the Flosolver is augmented further.

Results

The present computer code has been validated against a published calculation of an axisymmetric jet[18]. In addition, we have computed the divergence of the velocity at different times and found it to be of the same order as the computer precision. Since equation (6) can be solved without appeal to equation (7), the persistence of the divergence-free condition over time provides another indicator of the accuracy of the present simulation.

We present comparisons, in Figures 2 and 3, of the computed shape of the mean velocity distribution and wake thickness with measurements[7]. The agreement is seen to be reasonable; the thickness is slowly tending

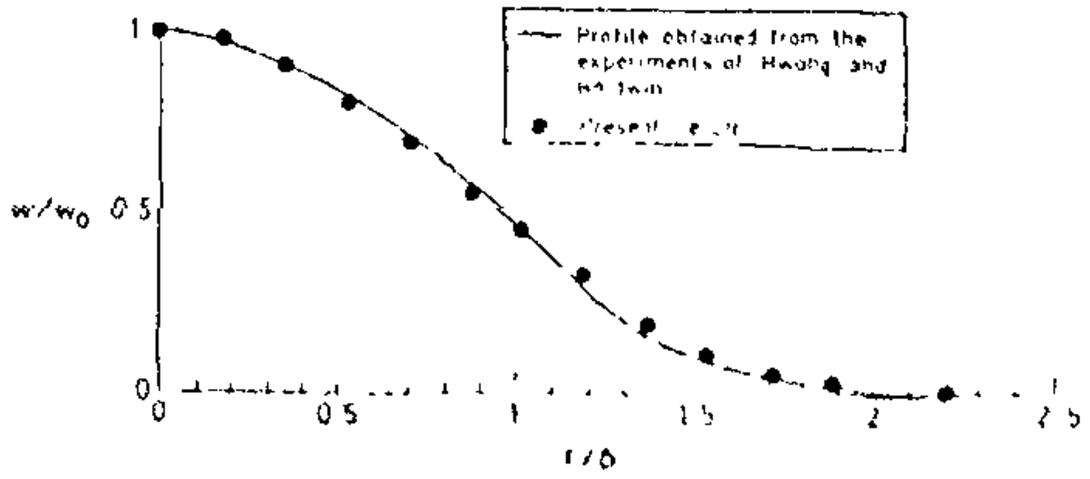

Figure 2. A comparison of the computed mean velocity defect profile with that in the experiments

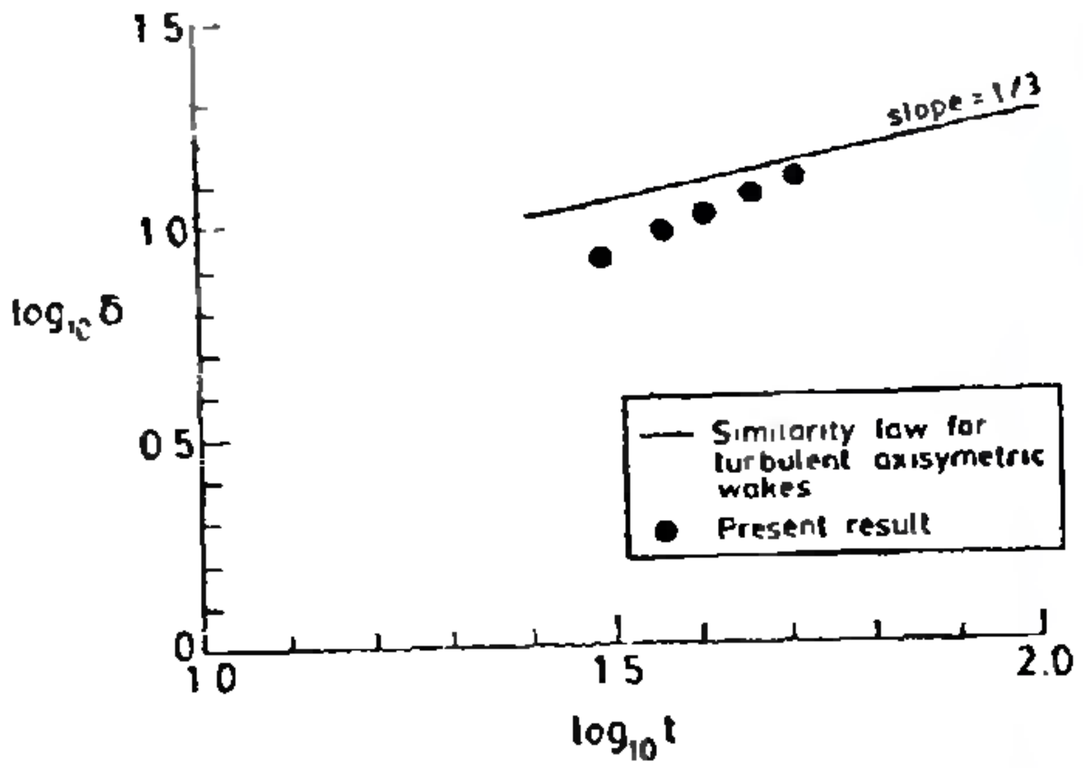

Figure 3. The computed growth of the wake along with the 'self-preserving' or 'similarity' solution.

towards the self-preserving solution, in a manner consistent with the slow approach observed in the experiments.

We now show some computer visualizations of the flow. When a selected variable is shown over the whole computational domain at some prescribed time, the picture is best interpreted as a representation of a short time history of the variable at a given station in z, this correspondence becoming more nearly exact as we move further downstream in the wake. In Figure 4 are shown two equivorticity surfaces (absolute magnitude) at time $t=5$. The initial shear layer has rolled up by this time into four vortex rings, which are *not* identical because of the streamwise perturbations imposed in modes $m=1, 2$ and 4 (see equation (11)). By time $t=20$ (Figure 5), the rings pair and there are essentially only two vortex rings in the domain. These rings develop an azimuthal instability in the manner studied by Widnall

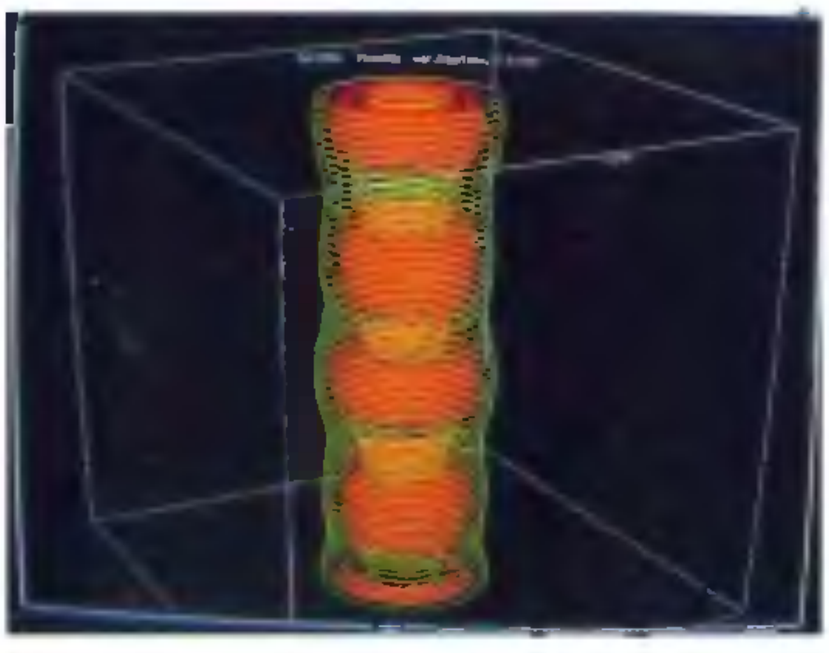

Figure 4. Surfaces of constant vorticity magnitude ω at time $t=5$ given by yellow ($\omega=0.5$) and red ($\omega=2.5$) (respectively about 10% and 50% of the peak vorticity observed at this time)

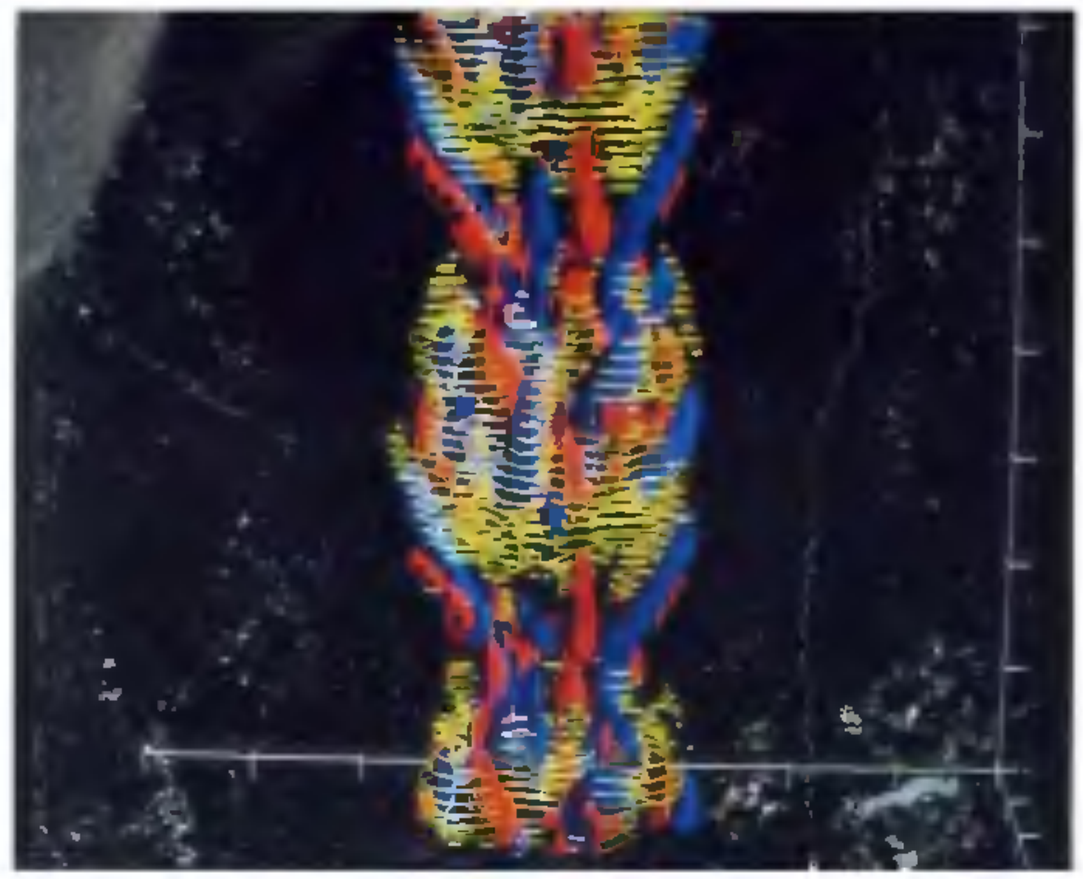

Figure 5. Surfaces of constant vorticity magnitude ω and streamwise vorticity ω_z at time $t=20$, yellow ($\omega=2$), red ($\omega_z=1$) and blue ($\omega_z=-1$).

et al.[19], and the strain field between the rings gives rise through longitudinal stretching to streamwise vortex structures. At later times (Figure 6) the vortex rings break down and the streamwise vortex structures dominate. At $t=50$, which is at the end of the present computations. the flow begins to show features indicative of fully developed turbulence, such as the emergence of small scales.

Figures 7*a*,*b* show typical streamwise and transverse sections of the vorticity distribution. Note that there are patches inside the wake where the flow is very nearly irrotational. The fractal nature of the edges is evident, and bears a strong qualitative resemblance to published pictures of jets[20]: no similar studies of axisymmetric

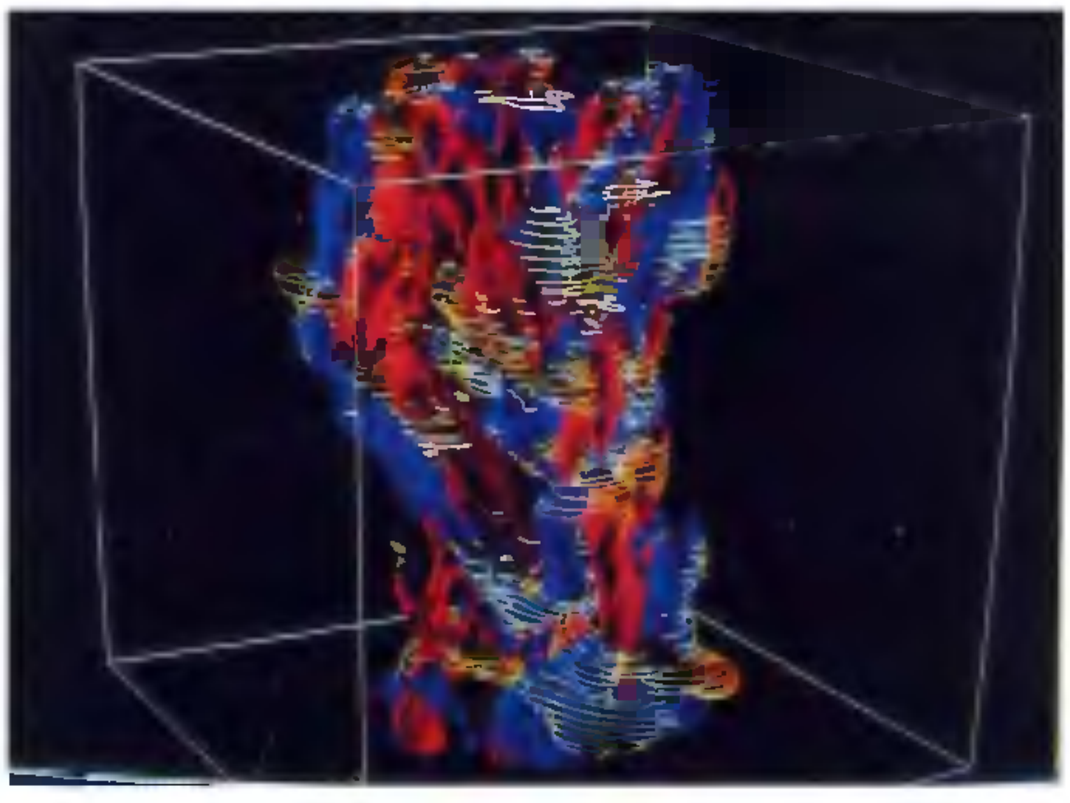

Figure 6. Surfaces of constant vorticity magnitude ω and streamwise vorticity ω_z at time $t=50$, yellow ($\omega=1$), red ($\omega_z=0.5$) and blue ($\omega_z=-0.5$)

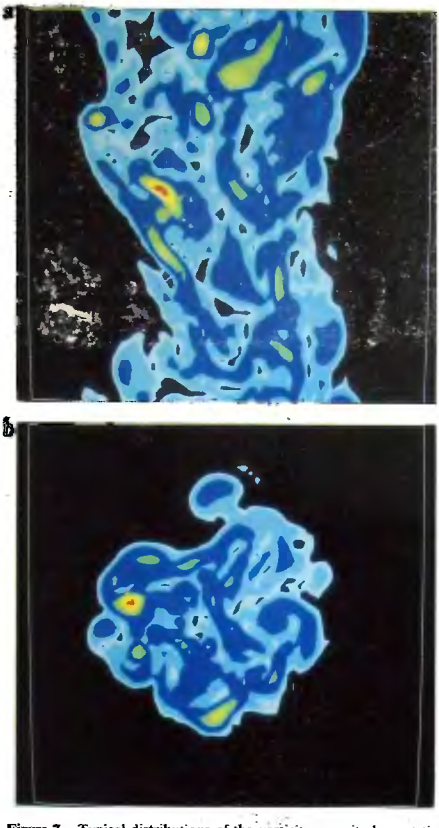

Figure 7. Typical distributions of the vorticity magnitude ω at time $t=50$ over a streamwise (*a*) and transverse (*b*) cross-section. In the figures, the vorticity strength increases from light blue ($\omega=0.25$) to red ($\omega=3$) in steps of 0.25.

wakes at moderate or high Reynolds numbers are known to us. Most reported flow-visualization studies[21,22] are limited to low Reynolds numbers (about 300 based on the macroscale), at which the near-wake shows helical instability. On the other hand, Simmons and Dewey[23] show pictures of the wake of a disk at a Reynolds number of about 5000, indicating nearly axisymmetric vortex shedding. In laboratory studies small non-axisymmetry or tunnel noise may trigger helical instabilities. In our computation no helical mode was initially excited, and the noise level is much less than that encountered in laboratory facilities; thus the initial axisymmetric vortex shedding and the absence of helical modes even at $t=50$ need occasion no surprise.

We finally present (Figure 8) an analysis of the evolution of the enstrophy $\Omega_i (=\int \omega_i^2$; $\bar{\omega}$ is the vorticity vector, and integration is over the whole computational domain). At $t=0$ the vorticity is entirely azimuthal; the total enstrophy $\Omega=\Sigma\Omega_i$ drops steeply with time as the initial shear layer grows, and reaches a minimum at $t\cong 12.5$. Around this time the streamwise enstrophy Ω_z starts becoming noticeable. Thereafter both Ω and Ω_z increase to a maximum, reached respectively at $t\cong 27$ and 30. At later times both enstrophies start dropping, but their ratio appears to be settling down to a nearly constant value of about 1/3, approaching equipartition. This non-monotonic variation of the component enstrophies as the flow evolves towards self-preservation adds an interesting twist to what has always been an intriguing problem.

Conclusion

We have presented a temporal simulation of the initial evolution of an axisymmetric wake at $\mathrm{Re}=1500$ on a 64^3 grid without any subgrid-scale turbulence modelling. Towards the end of the present simulation, the wake begins to show behaviour characteristic of turbulence, such as the emergence of small scales in the flow. To establish a self-preserving state (if indeed it exists) we need to continue the present calculations for a longer time, and this is being currently done.

The initial development of the wake reported here is qualitatively similar to what is known from laboratory studies of axisymmetric wakes[7,21–23]. At such early times, however, the evolution of the flow is strongly dependent on the precise initial conditions used, and one should not look for exact correspondence with any

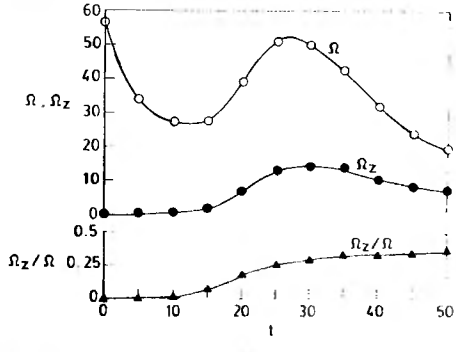

Figure 8. Evolution over time of the total enstrophy Ω, the streamwise enstrophy Ω_z and the ratio Ω_z/Ω

one experiment. The essential qualitative features such as formation of rings and their subsequent breakdown, along with the evolution of streamwise structures, are observed very clearly in the present simulation. The distinct advantage of such simulations is that, unlike in experiments, we are able to obtain accurate instantaneous pictures of the entire flow field.

1 Narasimha, R., in *Whither turbulence? Turbulence at the Crossroads* (ed Lumley, J. L.), Springer-Verlag, Heidelberg, 1990
2 Reynolds, W. C., in *Whither turbulence? Turbulence at the Crossroads* (ed Lumley, J. L.), Springer-Verlag, Heidelberg, 1990.
3 Canuto, C., Hussaini, M. Y., Quarteroni, A. and Zang, T. A., *Spectral Methods in Fluid Dynamics*, Springer-Verlag, New York, 1988.
4 Sinha, U. N. *et al*, Report No. PD ST 9133, NAL, Bangalore, 1991
5 Basu, A. J., Sinha, U. N. and Narasimha, R., Report No. PD CF 9213, NAL, Bangalore, 1992
6 Townsend, A. A., *The Structure of Turbulent Shear Flow*, Cambridge University Press, Cambridge, UK, 1956, 1976.
7 Hwang, N. H. C. and Baldwin, L. V., *J. Basic Eng.*, 1957, **88**, 261–268
8 Narasimha, R. and Sreenivasan, K. R., *Adv. Appl. Mech.*, 1979, **19**, 222–309
9 Orszag, S. A., *Stud. Appl. Math.*, 1971, **50**, 293–327.
10 Patterson, G. S. and Orszag, S. A., *Phys. Fluids*, 1971, **14**, 2538–2541.
11 Sinha, U. N., Deshpande, M. D. and Sarasamma, V. R., *Supercomputer*, 1989, **32**, 37–42
12 Pelz, R. B., *J. Comput. Phys.*, 1991, **92**, 296–312
13 Erlebacher, G., Bokhari, S. H. and Hussaini, M. Y., ICASE Report No. 87-41, 1987.
14 Tomboulian, S., Streett, C. L. and Macaraeg, M. G., ICASE Report No. 89-1, 1989
15 Basu, A. J., Technical Memorandum No. TM CF 9205, NAL, Bangalore 1992
16. Basu, A. J., *Parallel Computing* (submitted), 1992
17. Kerr, R. M., *J. Fluid Mech.*, 1985, **153**, 31–58.
18. Melander, M. V., Hussain, F. and Basu, A. J., in Proceedings of the 8th IUTAM symposium on turbulent shear flows, 1991.
19 Widnall, S. E., Bliss, D. B. and Tsai, C-Y., *J. Fluid Mech.*, 1974, **66**, 35–47.
20. Sreenivasan, K. R. and Meneveau, C., *J. Fluid Mech.*, 1986, **173**, 357–386.
21. Marshall, D. and Stanton, T. E., *Proc. R. Soc. London*, 1931, **A130**, 295–300
22 Roos, F. W. and Willmarth, W. W., *A.I.A.A. J.*, 1971, **9**, 285–287.
23. Simmons, L. F. G. and Dewey, N. S., A.R.C. R&M No. 1334, 1930.

ACKNOWLEDGEMENTS. We thank the Flosolver Team, without whose dedication to the parallel computing project the present computations would not have been possible. One of the authors, A.J.B., had been supported by a fellowship from the Jawaharlal Nehru Centre for Advanced Scientific Research during the initial part of this work.

Received 1 October 1992; accepted 9 October 1992